0026-895X/04/6603-580–591$20.00
MOLECULAR PHARMACOLOGY
Copyright © 2004 The American Society for Pharmacology and Experimental Therapeutics
Mol Pharmacol 66:580–591, 2004

Vol. 66, No. 3
3176/1170074
Printed in U.S.A.

Low Concentrations of Vinflunine Induce Apoptosis in Human SK-N-SH Neuroblastoma Cells through a Postmitotic G_1 Arrest and a Mitochondrial Pathway

Bertrand Pourroy, Manon Carré, Stéphane Honoré, Véronique Bourgarel-Rey, Anna Kruczynski, Claudette Briand, and Diane Braguer

Formation de Recherche en Evolution–Centre National de la Recherche Scientifique 2737, Université de la Méditerranée, Marseille, France (B.P., M.C., S.H., V.B.-R., C.B., D.B.); and Division of Experimental Cancer Research, Centre de Recherche Pierre Fabre, Castres, France (A.K.)

Received December 22, 2004; accepted June 1, 2004

This article is available online at http://molpharm.aspetjournals.org

ABSTRACT

Vinflunine, the newest fluorinated Vinca alkaloid, currently in phase III clinical trials, targets the microtubule network to induce mitotic block and apoptosis by mechanisms that remain unclear. In the current study, we investigated the apoptotic pathways induced by a wide range of vinflunine concentrations in SK-N-SH neuroblastoma cells. The concentrations of vinflunine that inhibited 50 and 70% of cell growth (IC_{50} and IC_{70}) induced high extents of apoptosis but failed to depolymerize microtubule network and to block cells in G_2/M. It is interesting that the IC_{50} and IC_{70} concentrations suppressed microtubule dynamics, slowed down mitotic progression from metaphase to anaphase, and induced a postmitotic G_1 arrest. This G_1 arrest was associated with an increase in p53 and p21 expression and with their nuclear translocation. A high concentration of vinflunine (500 nM) induced both microtubule depolymerization and a canonical G_2/M block. Mitochondria were involved in apoptotic pathways because all studied concentrations induced cytochrome *c* release. Bcl-2 family members were differently modulated by the different drug concentrations. Bax was up-regulated and translocated to mitochondria at the IC_{50} and IC_{70} concentrations, whereas Bcl-2 was phosphorylated only at the highest vinflunine concentration examined (500 nM). Our findings can be extended to other Vinca alkaloids, because similar results were obtained with vinblastine. All together, our results show that low concentrations of vinflunine fail to promote a G_2/M arrest but are sufficient to induce suppression of microtubule dynamics and subsequent apoptosis. Moreover, mitochondria constitute the point of convergence of apoptotic signals induced by both low and high concentrations of vinflunine.

Vinca alkaloids are major cancer chemotherapeutic drugs that affect microtubule integrity by inducing their destabilization. Vincristine (Oncovin), vinblastine (Velbe), and vinorelbine (Navelbine) are widely used in combination chemotherapy regimens for the treatment of solid tumors as well as for leukemia. Vinflunine (Javlor), the newest vinorelbine-derived drug, is a fluorinated compound obtained by superacid chemistry. It has demonstrated a marked antitumor activity in a panel of experimental tumor models (Kruczynski and Hill, 2001). Moreover, vinflunine is more active than vinorelbine, vinblastine, and vincristine against a number of murine tumors and human tumor xenografts (Kruczynski and Hill, 2001). Vinflunine is currently in phase III clinical trials.

This work was supported by Groupement des Entreprises Françaises dans la Lutte Contre le Cancer, Marseille-Provence.

Vinca alkaloids, including vinflunine, bind to α/β-tubulin dimers and microtubules and produce a remarkable range of effects that depend upon the drug concentration used (Kruczynski et al., 1998; Kruczynski and Hill, 2001; Ngan et al., 2001; Jordan, 2002). High concentrations of Vinca alkaloids cause extensive depolymerization of microtubules and formation of tubulin paracrystals. Lower concentrations induce depolymerization of the microtubule network, and the lowest effective concentrations suppress microtubule dynamics by reducing the rate of tubulin addition and loss at microtubule ends. Alterations of mitotic spindle functions by the Vinca alkaloids generally prevent cell cycle progression and lead to mitotic block (Kruczynski et al., 1998; Jean-Decoster et al., 1999; Ngan et al., 2001; Jordan, 2002). Vinflunine has some distinctive features relative to the other Vinca alkaloids. It binds to tubulin with severalfold lower overall affinity than

ABBREVIATIONS: MDA, microtubule-damaging agent; MTT, 3-[4,5-dimethylthiazol-2-yl]-2,5-diphenyltetrazolium bromide; FITC, fluorescein isothiocyanate; DAPI, 4.6-diamino-2-phenyndole; PI, propidium iodide; PBS, phosphate-buffered saline; BrdU, bromodeoxyuridine; FBS, fetal bovine serum.

vincristine or vinblastine (Lobert et al., 1998). Furthermore, the action of vinflunine on microtubule dynamics in vitro (i.e., both on dynamic instability and treadmilling) seems to differ significantly from that of vinblastine. The specific tubulin binding properties of vinflunine may account for its differential actions on microtubule dynamics (Ngan et al., 2000).

Vinca alkaloids, like other microtubule damaging agents (MDAs), are able to induce apoptosis in treated cells. Cells dying by apoptosis induced by the Vinca alkaloids exhibit typical morphological changes and DNA fragmentation. These drugs promote apoptosis in cancer cells through a complex process involving protein kinase signaling pathways, including activation of c-Jun NH_2-terminal kinase (Fan et al., 2000). Activation of several caspases by the Vinca alkaloids (Glaser and Weller, 2001; Liu et al., 2001; Groninger et al., 2002) leads to cleavage of one of their specific substrates, poly(ADP-ribose) polymerase, that is implicated in DNA repair (Liu et al., 2001). Mitochondria play a key role in apoptosis pathways by releasing apoptotic factors, including cytochrome *c*, that lead to apoptosome formation and then caspase activation. Mitochondria also seem to be involved in Vinca alkaloid-induced cell death. An increase in the production of mitochondrial reactive oxygen species and the loss of mitochondrial transmembrane potential occur in leukemic cells treated by vincristine (Groninger et al., 2002). In glioma cells, vincristine triggers cytochrome *c* release into cytosol, leading to apoptotic cell death (Glaser and Weller, 2001). We have demonstrated that vinorelbine directly affects mitochondria isolated from neuroblastoma cells, resulting in the release of cytochrome *c* (Andre et al., 2000). Mitochondrial Bcl-2-family members also have a critical role in Vinca alkaloid-induced apoptosis. An increase in the expression level of the apoptotic promoter Bax and a down-regulation of the apoptotic suppressor Bcl-2 are associated with treatment of various cancer cell lines with vincristine (Kawakami et al., 1999; Wall et al., 1999). Furthermore, vinorelbine and vinblastine induce Bcl-2 inactivation by phosphorylation and then promote apoptosis of treated cells (Fan et al., 2000; Liu et al., 2001). Little is known about the pro-apoptotic effect of vinflunine. It has been shown that vinflunine-induced apoptosis was mediated by caspase-3 and/or -7 and poly(ADP-ribose) polymerase cleavage (Kruczynski and Hill, 2001). Moreover, vinflunine can induce Bcl-2 phosphorylation, a capacity that seems to depend on the cell type. Bcl-2 family members may play a role in the overall cellular response to vinflunine treatment, because vinflunine-resistant P388 cells are characterized by a relatively high level of expression of the antiapoptotic proteins Bcl-2 and Bfl1/A1 (Kruczynski and Hill, 2001; Kruczynski et al., 2002). Several aspects of the apoptotic pathways triggered by Vinca alkaloids remain unclear. Vinca alkaloids and the other MDAs are described to induce a G_2/M arrest before apoptosis, but the molecular mechanisms that link mitotic arrest and apoptosis are poorly understood. In addition, mitotic block, a hallmark property of these drugs, is not always observed, and other cell cycle modifications can occur (Blajeski et al., 2002).

We show a new mechanism of action of vinflunine at low concentrations in human neuroblastoma SK-N-SH cell line. This drug, at concentrations that inhibit cell growth by 50 or 70%, induced a high extent of apoptosis after a postmitotic G_1 arrest that was associated with microtubule dynamics suppression and p53 and p21 up-regulation. As expected, high concentrations of vinflunine blocked SK-N-SH cells at mitosis before apoptosis. Finally, this study demonstrates that, whatever the concentration, mitochondria are the point of convergence for the apoptotic signals induced by the Vinca alkaloids.

Materials and Methods

Cell Culture and Drug Treatment. Human neuroblastoma SK-N-SH, SH-SY5Y, IMR 32, and SHEP cells were maintained at 37°C and 5% CO_2 in standard culture RPMI 1640 medium containing 10% fetal bovine serum (FBS), 2 mM glutamine, 1% penicillin, and streptomycin. Exponentially growing cells were seeded at 10^5 cells/ml for SK-N-SH, SH-SY5Y, and IMR32 cells and 10^4 cells/ml for SHEP cells, 3 days before drug treatment as described previously (Andre et al., 2000).

The immortalized mammary HBL-100 cells were seeded at 0.5×10^5 cells/ml and maintained at 37°C and 5% CO_2 in Dulbecco's modified Eagle's medium with 10% FBS, glutamine, penicillin, and streptomycin, and 1% sodium pyruvate. The colon adenocarcinoma LoVo cells were seeded at 1.5×10^5 cells/ml and maintained at 37°C and 5% CO_2 in RPMI-1640 medium with 10% FBS, 2 mM glutamine, 1% penicillin, and streptomycin.

The ratio drug molar concentration/cell number is strictly identical for all the experiments. Stock solutions of vinflunine (Pierre Fabre Oncologie, Castres, France), vinblastine (Lilly, Saint Cloud, France) and vinorelbine (Pierre Fabre Oncologie, Castres, France) were prepared in distilled water

Cytotoxicity Assays. Growth inhibition of cells was studied after a 72-h treatment with drugs by using the MTT cell proliferation assay as described previously (Carles et al., 1998). The IC_{50} and IC_{70} were graphically determined.

Detection of Apoptosis by Annexin-V-FITC and DAPI Staining. Surface exposure of phosphatidylserine in apoptotic cells was measured by using Annexin V-FITC staining (Euromedex, Souffelweyersheim, France). After a 72-h treatment, supernatant and adherent cells were exposed to Annexin-V-FITC and propidium iodide (PI; Fluka, Steinheim, Germany) for 15 min before flow cytometry analysis (FACScan; BD Biosciences, San Jose, CA) as described previously (Gonçalves et al., 2000). Apoptosis was also detected by DAPI staining (Sigma Aldrich, Steinheim, Germany), and the percentages of apoptotic cells, defined by the condensation of nuclear chromatin and nuclear fragmentation, were quantified.

Cell Cycle Analysis and BrdU Incorporation Assay. To perform cell cycle analysis, cells treated for 24 h were harvested, fixed in ice-cold methanol, and incubated with PI immediately before analysis. DNA content was measured by flow cytometry. Cytogram analysis was performed with Mod Fit software (BD Biosciences, Mississauga, Canada) as described previously (Chen and Horwitz, 2002). The mitotic indices were determined, after DAPI staining, by quantification of the mitotic cells in control cells and in cells treated by the IC_{50}, the IC_{70}, and 500 nM concentrations of vinflunine for 6, 12, and 24 h. Mitotic indices represent counts of at least 1000 cells from three independent experiments. We also quantified the distribution of mitotic cells after a 24 h treatment in the different phases of mitosis (i.e., prometaphase, metaphase, and anaphase). The anaphase/metaphase ratio, calculated by dividing the number of cells in anaphase by the number of cells in prometaphase and metaphase, was determined to evaluate the transition of cells from metaphase to anaphase.

For BrdU incorporation study, cells were pulsed with 20 μM BrdU for 30 min at 37°C before treatment or after a 24-h drug treatment. Twenty-four hours later, cells were resuspended in 70% ice-cold methanol and fixed for 30 min on ice. Cells were then denatured by incubation with 2 N HCl for 30 min at room temperature. After

centrifugation, the pellet was resuspended in 0.1 M $Na_2B_4O_7 \cdot 10H_2O$, pH 8.5, to neutralize the acid. Cells in 50 μl of 0.5% PBS/Tween 20 were first incubated with a primary anti-BrdU antibody (BD Biosciences) for 30 min at 4°C and then with a secondary FITC-conjugated antibody (Jackson Immunoresearch Laboratories, Baltimore, MD). Finally, cells were resuspended in PBS containing 5 μg/ml PI and analyzed by flow cytometry.

Cell Fractionation and Western Blotting. Nuclei and mitochondria were isolated from SK-N-SH as described previously (Carre et al., 2002). To obtain a cytosolic extract, cells were washed in PBS and lysed by incubating for 30 s in lysis buffer (75 mM NaCl, 8 mM Na_2HPO4, 1 mM NaH_2PO4, 1 mM EDTA, and 350 μg/ml digitonin). The lysates were then centrifuged at 15,000*g* for 10 min at 4°C, and the supernatants were collected as described previously (Andre et al., 2002).

Cells, nuclei, or mitochondria were resuspended in lysis buffer specific to the studied proteins. To detect phosphorylated Bcl-2, radioimmunoprecipitation assay buffer (2 mM EDTA, 100 mM NaCl, 1 mM Na_3VO_4, 1% Triton X-100, and 50 mM Tris-HCl, pH 7.5) was used. For other studies (p53, p21, Bax, Bcl-2, cytochrome *c*), whole cells or extracts were sonicated in a lysis buffer (62.5 mM Tris base, pH 6.8, 2% SDS, 50 mM dithiothreitol, and 10% glycerol) and boiled for 5 min. Equal amounts of the proteins were separated by using 10%–15% SDS-polyacrylamide gel electrophoresis and electrotransferred onto a nitrocellulose membrane. Membranes were then blocked in 5% nonfat milk in PBS and then probed with different antibodies. Visualization of the proteins was then accomplished using an enhanced chemiluminescence detection kit (Amersham Biosciences, Little Chalfont, Buckinghamshire, UK) as described previously (Carre et al., 2002). The primary antibodies used were anti p53 (1:100; mouse monoclonal, DakoCytomation, Glostrup, Denmark), p21/WAF1(Ab-1) (1:100; mouse monoclonal, Calbiochem, San Diego, CA), Bax (1:50; mouse monoclonal, Santa Cruz Biotechnology, Santa Cruz, CA), Bcl-2 (1:100; mouse monoclonal, DakoCytomation), and cytochrome *c* (1:500; mouse monoclonal, BD PharMingen, San Diego, CA). Peroxidase conjugated goat anti-mouse antibodies were used as secondary antibodies (Jackson Immunoresearch Laboratories).

Immunofluorescence Staining. Cells were grown on eight-well plates (Labtek, Naperville, IL) and incubated with the different Vinca alkaloids. Cells were then fixed with 3.7% formaldehyde, permeabilized with 1% saponin, and successively incubated with primary antibody: anti-α-tubulin (1:400, mouse monoclonal; Sigma-Aldrich, Steinheim, Germany), anti-p53 (1:50, mouse monoclonal; DakoCytomation), or anti-cytochrome *c* (1:25, mouse monoclonal; BD PharMingen, San Diego, CA) antibodies and secondary antibody conjugated with FITC (Jackson Immunoresearch Laboratories) as described previously (Andre et al., 2002). Cells were observed using a Leica DM-IRBE microscope, 100× objective lens, coupled with a digital camera (Coolsnap FX; Princeton Instruments, Trenton, NJ). Four hundred cells were analyzed with Metamorph software (Universal Imaging Corporation, Downingtown, PA) for each experiment, performed in triplicate.

Microinjection of Rhodamine-Labeled Tubulin. Tubulin was purified from lamb brain by sulfate fractionation and ion-exchange chromatography. The protein was stored in liquid nitrogen and prepared as described previously (Barbier et al., 2001). The labeling by tetraethyl rhodamine succinimidyl ester (Molecular Probes, Leiden, Netherlands) of tubulin in the assembled form (as microtubules) was based on the protocols described previously (Mejillano and Himes, 1989; Hyman et al., 1991) using a phosphate/glycerol assembly buffer (10 mM NaP_i, 1 mM EGTA, 3.4 M glycerol, 6 mM $MgCl_2$, and 0.5 mM GTP, pH 6.9). Labeled tubulin was stored in 30-μl aliquots in liquid nitrogen until use. SK-N-SH cells were seeded 72 h before use on glass coverslips. Rhodamine-tubulin was centrifuged at 35,000 rpm for 15 min at 4°C to remove aggregates. Rhodamine–tubulin was diluted by a third in buffer (2 mM Tris-acetate, pH 7, 50 mM KCl, and 0.1 mM 1,4-dithioerythritol) to obtain a 5 mg/ml final concentration just before microinjection into SK-N-SH cells using a Femtojet and micromanipulator 5171 (Eppendorf AG, Hamburg, Germany). Injected cells were incubated 2 h at 37°C to allow for incorporation of rhodamine-tubulin into microtubules and further incubated with vinflunine for 4 h to allow attainment of an equilibrium intracellular drug concentration.

Time-Lapse Microscopy and Image Acquisition. Microinjected cells were placed in RPMI culture medium lacking sodium bicarbonate and supplemented with 25 mM HEPES, 4.5 g/l glucose, 30 μl of Oxyrase/ml (Oxyrase Inc., Mansfield, OH) to reduce photodamage, in a double-coverslip chamber maintained at 37 ± 1°C, and observed using a fluorescence microscope (Leica DM-IRBE) with a 100× objective lens. Thirty-one images per cell were acquired at 4-s intervals using a digital camera (Coolsnap FX; Princeton Instruments) driven by Metamorph software (Universal Imaging Corporation).

Analysis of Microtubule Dynamic Instability. Analysis of microtubule dynamic instability was performed as described previously (Gonçalves et al., 2001; Honoré et al., 2003). The positions of the plus-ends of individual microtubules with time were recorded and analyzed by using Metamorph software (Universal Imaging Corporation). The lengths of individual microtubules were graphed as a function of time (life histories). Changes in length $\geq$0.5 μm were considered growth or shortening events. Changes in length $<$0.5 μm were considered phases of attenuated dynamics or pause. The rates of growth and shortening were determined by linear regression. Means and standard errors (S.E.) were calculated per event. The catastrophe frequency based on time was calculated by dividing the number of transitions from growth or pause to shortening by the total time growing and paused for each individual microtubule. The rescue frequencies based on time were calculated similarly by dividing the total number of transitions from shortening to pause or growth by the time spent shortening for each individual microtubule. Means and SE of transition frequencies were calculated per microtubule (n = 35 for each experimental condition). Dynamicity is the total length grown and shortened divided by the life span of the population of microtubules (Toso et al., 1993).

RNA Isolation and RT-PCR Analysis. Total cellular RNA was prepared with the High Pure RNA isolation kit (Roche Diagnostics, Mannheim, Germany). One microgram of total RNA was used for reverse transcription with random primers. Then RNAs of p53 and β_2 microglobulin (β_2m), the internal standard, were amplified with *Taq* polymerase (Eurobio, Les Ulysses, France). The primer sequences were: p53: sense, 5′-CTG AGG TTG GCT CTG GAC TGT ACC ACC ATC C-3′; antisense, 5′-CTC ATT CAG CTC TCG GAA CAT CTC GAA GCG-3′ and β2m: sense, 5′-CCGACATTGAAGTTGACTTAC-3′; antisense, 5′-ATCTTCAAACCTCCATGATG-3′.

PCR was carried out in a PerkinElmer system 2400 (PerkinElmer Life and Analytical Sciences, Courtaboeuf, France). The reaction conditions included a denaturation at 94°C for 5 min, followed by 22 (for β2m) or 25 (for p53) cycles of denaturation at 94°C for 30 s, annealing 30 s at 60°C, extension at 72°C for 45 s, and one final cycle of extension at 72°C for 7 min. The amplified products were separated by electrophoresis on a 2% agarose gel. The DNA bands were visualized by ethidium bromide staining (Sigma-Aldrich), and the image was digitized. p53 expression was normalized to β2m transcript. This was noted as the relative expression level, which equals the densitometric value of p53/densitometric value of β2m.

Statistical Analysis. Sigma Stat software (Jandel Scientific, San Rafael, CA) was used to perform statistical analysis. Each experiment was performed at least in triplicate. Statistically significant difference between two conditions was retained for $p < 0.05$.

Results

Vinflunine Induces Apoptosis in Neuroblastoma SK-N-SH Cells. The effects of a range of vinflunine concentrations on SK-N-SH cell proliferation were compared with

those of vinorelbine and vinblastine, using an MTT assay. Vinflunine inhibited cell growth in a concentration-dependent manner (Fig. 1A). After a 72-h treatment, vinflunine, vinorelbine, and vinblastine inhibited 50% cell growth (IC_{50}) at 50, 13.5, and 2 nM, respectively. The IC_{70} values for the same drugs were 80, 30, and 3.7 nM, respectively. These results are consistent with previous data obtained on different tumor cell lines (Kruczynski et al., 1998).

The following experiments were performed at two low concentrations (at the IC_{50} and the IC_{70}) and at one high concentration (500 nM), which exhibited a maximum cytotoxic effect for the three drugs. All studied vinflunine concentrations are clinically relevant, in that concentrations in the plasma of patients are higher than 9 μM for the recommended dose of 320 mg/m^2 (Bennouna et al., 2003).

To investigate whether inhibition of cell growth in the SK-N-SH cells by vinflunine was caused by apoptosis, we performed Annexin-V-FITC staining at 72-h of treatment. As shown in Fig. 1B, vinflunine treatment induced apoptosis in a concentration–dependent manner (64 ± 12, 85 ± 8, and 94 ± 2% for the IC_{50}, IC_{70}, and 500 nM concentrations, respectively). The increase in the percentage of apoptotic cells relative to the drug concentration was further confirmed by DAPI staining (Fig. 1C). Thus, inhibition of cell growth by vinflunine is associated with an apoptotic mechanism at all studied concentrations.

Low Concentrations of Vinflunine Induce Apoptosis without G_2/M Arrest. Vinca alkaloids are known to induce depolymerization of the microtubule network and a G_2/M block in proliferating cells. Apoptosis is generally detected from 24 to 48 h later.

We investigated whether the IC_{50} and IC_{70} for vinflunine could induce a G_2/M block after a 24-h treatment. The con-

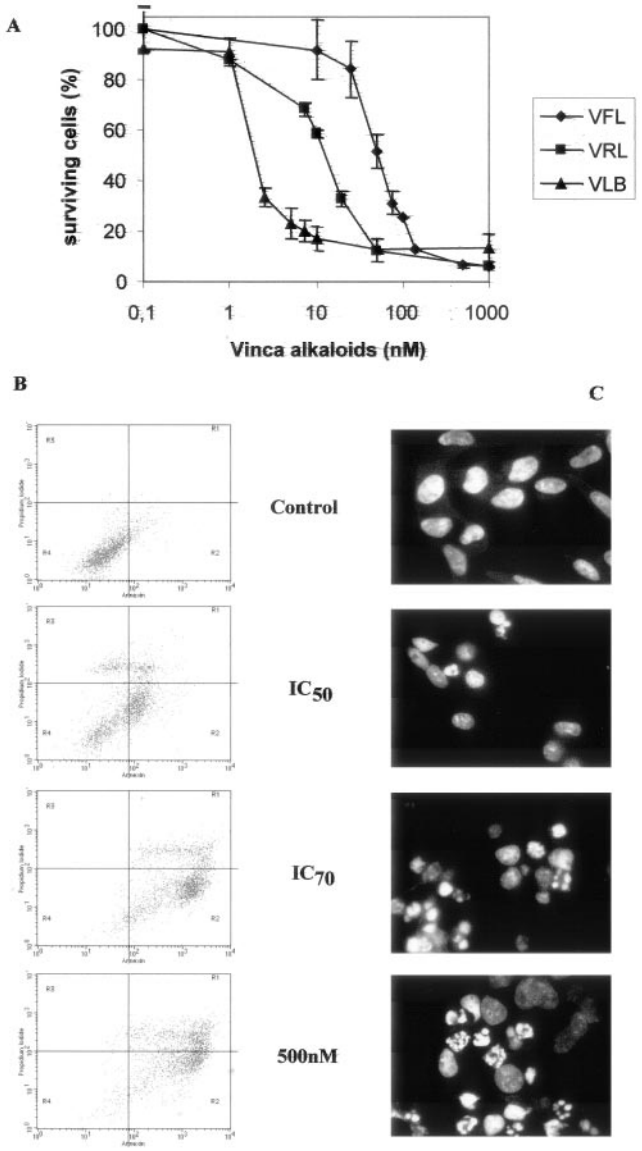

Fig. 1. Vinflunine induces apoptosis of neuroblastoma SK-N-SH cells. A, concentration dependence for inhibition of cell growth by vinflunine (♦) compared with vinblastine (▲) and vinorelbine (■). Exponentially growing cells were incubated with the drugs for 72 h, and cell proliferation was assessed by using the MTT reagent. Results represent means ± S.D. of at least three independent experiments. B, cytograms of cells stained with Annexin V-FITC and propidium iodide (PI) dual labeling after a 72-h treatment. Apoptotic and late apoptotic cells are located in gates R1 and R2. C, DAPI staining of cells visualized by fluorescent microscopy. Apoptotic cells contain fragmentized nuclei. The cells were incubated with the IC_{50}, the IC_{70}, or 500 nM vinflunine for 72 h before staining. Cytograms and micrographs are representative of three independent experiments.

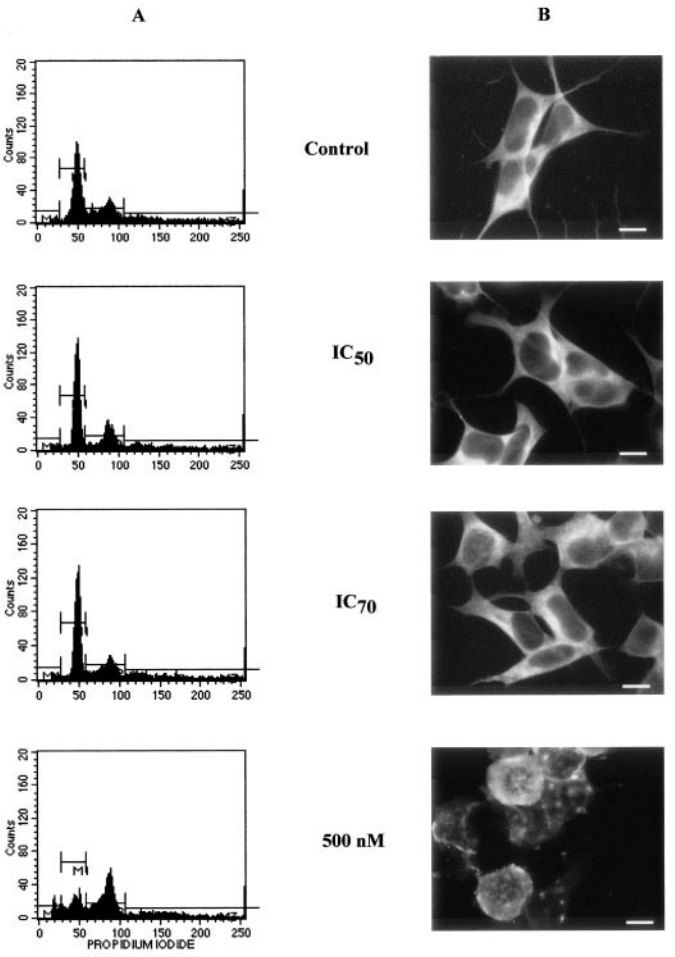

Fig. 2. Apoptosis is related to microtubule depolymerization and G_2/M arrest only at high concentrations of vinflunine. A, DNA distribution in cells treated with IC_{50}, IC_{70}, or 500 nM vinflunine for 24 h. The cells were stained with PI and analyzed by flow cytometry. Histograms and pictures are representative of three independent experiments. B, microtubule network visualization by fluorescent microscopy. The cells were treated with IC_{50}, IC_{70}, or 500 nM vinflunine for 24 h and stained with α-tubulin antibody. Scale bar, 5 μm.

centration dependence of G_2/M arrest at 24 h of treatment is shown in Fig. 2A. Only the high concentrations of vinflunine (500 nM) blocked the cell cycle in the G_2/M phase. Quantification of cells in G_2/M and interphase with Mod Fit confirmed both the high proportion of G_2/M cells after the treatment with 500 nM vinflunine (59 ± 11 versus 16 ± 4% for control) and the absence of a G_2/M block in cells treated with the IC_{50} and IC_{70} concentrations of vinflunine (22 ± 2% and 26 ± 3% of G_2/M cells, respectively; there was no statistical difference with control, $p > 0.05$). No G_2/M block occurred at the IC_{50} or IC_{70} concentration after shorter or longer treatment (12–48 h) (data not shown).

To examine the effects of vinflunine on the microtubule network in SK-N-SH cells, we performed comparative immunostaining of α-tubulin in control cells and in cells treated for 24 h with the IC_{50}, the IC_{70}, and the high concentration (500 nM) of vinflunine. Only the high-vinflunine concentration induced the expected microtubule depolymerization and the rounding of the cells (Fig. 2B). It was surprising that the IC_{50} and IC_{70} concentrations of vinflunine induced neither modification of the cell shape nor changes in the appearance of the microtubule network (Fig. 2B). Thus, low concentrations (IC_{50} or IC_{70}) of vinflunine may induce apoptosis in the neuroblastoma SK-N-SH cell line without previous depolymerization of microtubule network and G_2/M block.

Apoptosis without G_2/M Block Induced by Low Concentrations of Vinflunine Is Specific to Neuroblastoma Cells. To investigate whether apoptosis without G_2/M block is specific to SK-N-SH cells, we tested this paradigm in cell lines, from both neural and non-neural origin.

First, we tested vinflunine in non-neuronal cells. Vinflunine concentrations that inhibited 50% of cell growth at 72 h of treatment were 60 and 75 nM for the nontumoral mammary HBL-100 cells and for colon adenocarcinoma LoVo cells, respectively. As shown in Fig. 3, A and B, the IC_{50} concentrations of vinflunine induced massive G_2/M block in both cell lines, compared with untreated cells. We also tested a high concentration (500 nM) that exhibits a maximum cytotoxic effect of vinflunine and observed a G_2/M block for HBL-100 and LoVo cells (Fig. 3C). We checked that IC_{50} concentrations of vinflunine induced apoptosis after a 72-h treatment in both cell lines as shown in Fig. 3D. Thus, contrary to SK-N-SH cells, IC_{50} concentrations of vinflunine induce a canonical G_2/M block and subsequent apoptosis in non-neuronal cell lines.

Then, we tested other neuroblastoma cell lines: IMR 32 cell line and the two SK-N-SH subclones (i.e., Schwann cell-like SHEP cells and neural SH-SY5Y cells). The IC_{50} concentrations of vinflunine at 72 h of treatment were 30, 55, and 20 nM for SHEP, SH-SY5Y, and IMR32 cells, respectively. As

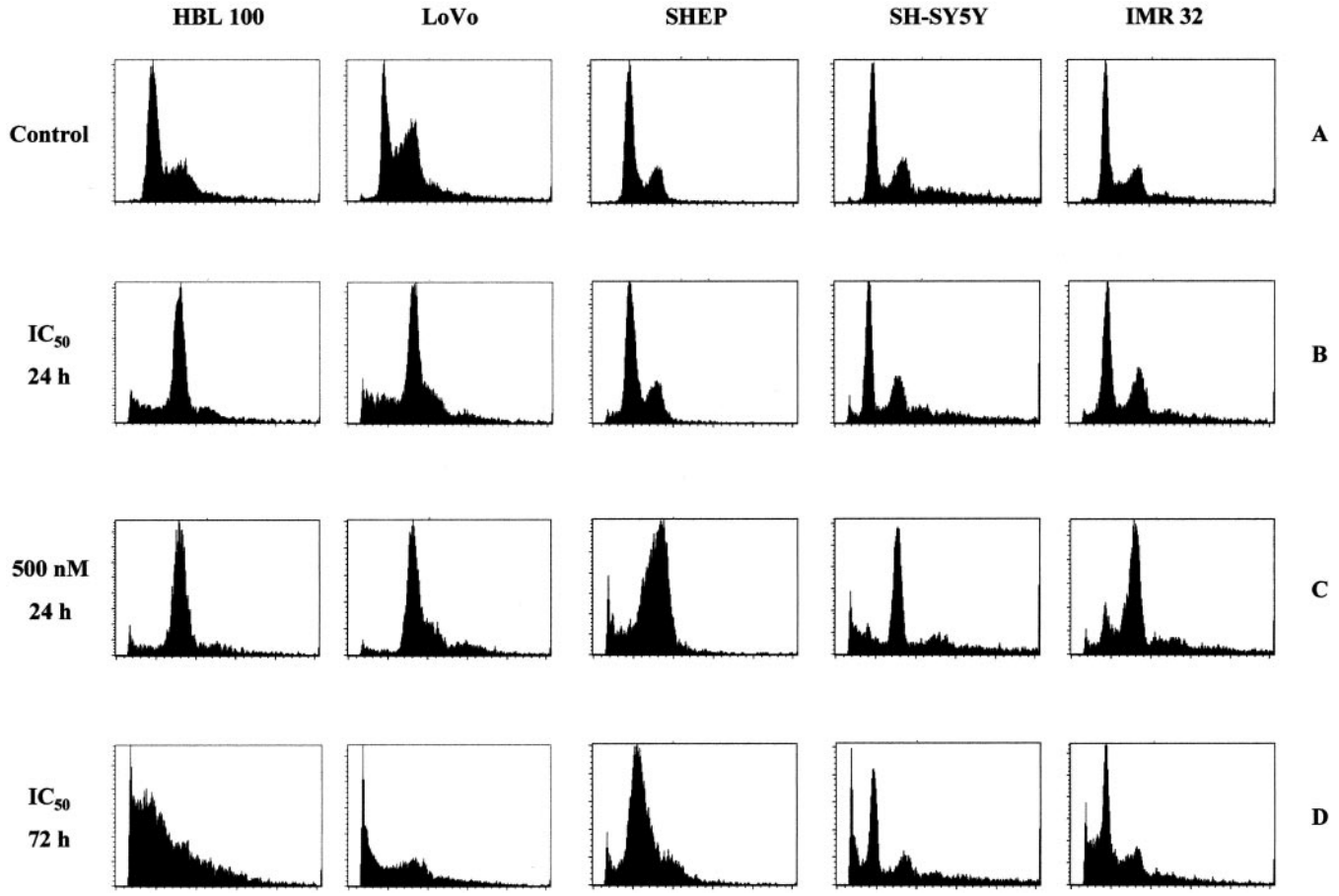

Fig. 3. Apoptosis without G_2/M block is specific to neuroblastoma cells. HBL-100, LoVo, SHEP, SH-SY5Y, and IMR32 cells were stained with PI and analyzed by flow cytometry. Histograms are representative of three independent experiments. DNA distribution in: control cells (A), cells treated by IC_{50} of vinflunine for 24 h (B), cells treated by 500 nM of vinflunine for 24 h (C), and cells treated by IC_{50} of vinflunine for 72 h (D). Sub-G_1 peak, corresponding to DNA fragmentation is related to apoptosis.

shown in Fig. 3, A and B, for the three neuroblastoma cell lines, the IC_{50} concentrations of vinflunine failed to induce G_2/M block after a 24-h treatment, whereas a high concentration of 500 nM induced a canonical G_2/M block (Fig. 3C). For the three neuroblastoma cell lines, the IC_{50} concentrations of vinflunine induced apoptosis after a 72-h treatment. Thus, we showed that apoptosis without G_2/M block induced by vinflunine is specific to neuroblastoma cells.

Low Concentrations of Vinflunine Suppress Microtubule Dynamics and Slow Mitotic Transition. To understand how vinflunine acts at low concentrations in neuroblastoma cells, we investigated whether vinflunine affects microtubule dynamics in living cells as described for other MDAs (Jordan, 2002).

We microinjected living SK-N-SH cells with rhodamine-labeled tubulin and observed the dynamic properties of their microtubules by time-lapse fluorescence microscopy after a treatment by the IC_{50} concentration of vinflunine. In control cells, microtubules alternated between phases of growing, shortening, and pause states (a state of attenuated dynamic instability). As shown in Table 1, the plus ends of control microtubules grew at a mean rate of 9.2 ± 0.5 μm/min, slower than their mean shortening rate of 12.6 ± 0.9 μm/min. The mean lengths grown and shortened were 1.6 ± 0.1 and 1.8 ± 0.1 μm, respectively. Microtubules spent half of their time (46.2%) in a paused state, neither growing nor shortening to a detectable extent. The overall microtubule dynamicity (see *Materials and Methods*) was 5.8 μm/min. It was interesting that low concentrations of vinflunine (at the IC_{50}) reduced the overall microtubule dynamicity by 34.8% compared with untreated cells (3.8 and 5.8 μm/min, respectively). Vinflunine reduced the rates of growth and shortening (19% and 29%, respectively), and the lengths grown and shortened (23% and 15.5%, respectively) (Table 1). Thus, low concentrations of vinflunine can induce apoptosis with suppression of microtubule dynamics.

Subtle suppression of microtubule dynamics inhibits the function of the mitotic spindle, thereby slowing cell cycle progression at the metaphase/anaphase transition (Jordan et al., 1996). Thus, we closely investigate the impact of low concentrations of vinflunine on mitosis although we did not detect G_2/M block.

First, we quantified the mitotic index. As shown in Table 2, both the IC_{50} and IC_{70} concentrations of vinflunine slightly increased the percentage of cells in mitosis [4.3 ± 0.8% for control cells versus 6.2 ± 0.9% ($p > 0.05$) and 9.8 ± 1.8% ($p < 0.05$) for cells treated by the IC_{50} and IC_{70} concentrations, respectively]. Moreover, we can observe that the mitotic index remained constant from 6 to 24 h treatment by the IC_{50} and IC_{70} concentrations of vinflunine. These data suggest that this low increase in mitotic index proceeded from a slower mitotic transition. Then, we quantified anaphase/metaphase ratio in control cells and cells treated for 24 h with vinflunine. As shown in Table 2, the slight increase in mitotic index was related to a slowing down of the progression into mitosis as shown by the decrease in anaphase/metaphase ratio (from 0.19 ± 0.02 for control to 0.03 ± 0.01 for IC_{70}). Furthermore, neither aneuploid nor multinucleated cells, resulting from an aberrant mitosis, were detected by analyzing the DNA content profiles by Mod Fit and DAPI

TABLE 1
Vinflunine inhibits microtubule dynamics in living SK-N-SH cells
Results are expressed as mean ± S.E.M. of 35 microtubules analysis per condition.

Parameters	Control	VFL (50 nM)	Percentage Change
Overall Dynamicity (μm/min)	5.8	3.8	−34.8%
Rate (μm/min)			
Growing	9.2 ± 0.5	7.5 ± 0.2*	−19%
Shortening	12.6 ± 0.9	8.9 ± 0.2**	−29%
Mean length (μm)			
Growing	1.6 ± 0.1	1.2 ± 0.1**	−23%
Shortening	1.8 ± 0.1	1.5 ± 0.1**	−15.5%
Mean duration (min)			
Growing	0.17 ± 0.01	0.16 ± 0.01	N.S.
Shortening	0.15 ± 0.01	0.17 ± 0.01*	+13%
Attenuation	0.21 ± 0.02	0.26 ± 0.03	N.S.
Transition frequencies (min^{-1})			
Catastrophe	2.5 ± 0.3	2.2 ± 0.3	N.S.
Rescue	7.2 ± 0.7	6.2 ± 0.6	N.S.

* $P < 0.05$.
** $P < 0.01$.
N.S., not significant.

TABLE 2
Vinflunine increases mitotic index and inhibits metaphase to anaphase transition
Results are expressed as mean ± S.D. (counting of 1000 cells per condition).

	Mitotic Index			Anaphase/Metaphase ratio
	6 h	12 h	24 h	24 h
		%		
Control	3.7 ± 0.5	4.2 ± 0.5	4.3 ± 0.8	0.19 ± 0.02
IC_{50}	6.3 ± 2.4	6.8 ± 1.5	6.2 ± 0.9	0.12 ± 0.04*
IC_{70}	7.1 ± 1.6	9.8 ± 2.6	9.8 ± 1.8*	0.03 ± 0.01*
500 nM	9.4 ± 3.5*	28 ± 4.2**	40.6 ± 1.0**	0.00 ± 0.00*

* $P < 0.05$.
** $P < 0.01$.

staining, suggesting that cells treated at the IC_{50} and IC_{70} succeeded in exiting from a slower mitosis.

In contrast, high concentration (500 nM) of vinflunine increased the mitotic index massively after 24 h of treatment (41 ± 1%). We observed an accumulation in mitosis of the cells treated by this high concentration from 6 to 24 h (Table 2). In addition, 500 nM vinflunine totally abolished the transition from metaphase to anaphase because cells were blocked in a metaphase-like state and no anaphases were detected.

Together, these data suggest that low concentrations of vinflunine may induce a high degree of apoptosis through a mechanism that is associated with suppression of microtubule dynamics and a slower cell cycle progression, without accumulation of cells in mitosis. In contrast with low concentrations of vinflunine and as usually described, the high concentration of vinflunine seems to trigger apoptosis via microtubule depolymerization and mitotic block.

Low Concentrations of Vinflunine Induce a Postmitotic G_1 Arrest Associated with Up-Regulation of p53 and p21. To understand how suppression of microtubule dynamics leads to apoptosis, we investigated cell cycle progression beyond 24 h treatment. We performed a BrdU incorporation study to search for a possible postmitotic arrest in G_1 phase. Because BrdU incorporation is a test of DNA synthesis and thus transition of cells through S phase, we observed the cell cycle distribution of BrdU-labeled or nonlabeled cells after 48-h treatment by vinflunine (at the IC_{50} and IC_{70}). We pulsed cells with BrdU after a 24-h treatment by vinflunine and quantified cells with a 2n DNA content (i.e., in G_1 phase) 24 h later. As shown in Fig. 4B, the percentage of BrdU nonlabeled cells in G_1 strongly increased after the treatment with the IC_{50} or IC_{70} concentrations of vinflunine (35 ± 8% and 50 ± 4%, respectively) compared with control cells (11 ± 2%). These results indicate that vinflunine inhibits the progression of cells from G_1 to S. Thus, cells treated with the IC_{50} or the IC_{70} of vinflunine seem to normally exit from mitosis and then undergo a postmitotic G_1 arrest.

To check that no G_1 arrest occurred before the slowing down of mitosis and exiting from it, we pulsed cells with BrdU before drug addition and observed the cell-cycle distribution after a 24-h treatment by vinflunine. As shown in Fig. 4A, the percentage of G_1 BrdU-labeled cells treated at the IC_{50} or the IC_{70} with vinflunine and in control cultures was very similar (33 ± 3, 32 ± 6, and 30 ± 1% respectively; $p > 0.05$). Thus, low concentrations of vinflunine did not induce a premitotic G_1 arrest.

Induction of p53 is known to block cells in interphase after a cellular stress or DNA injury. To investigate whether p53 was involved in the postmitotic G_1 arrest induced by vin-

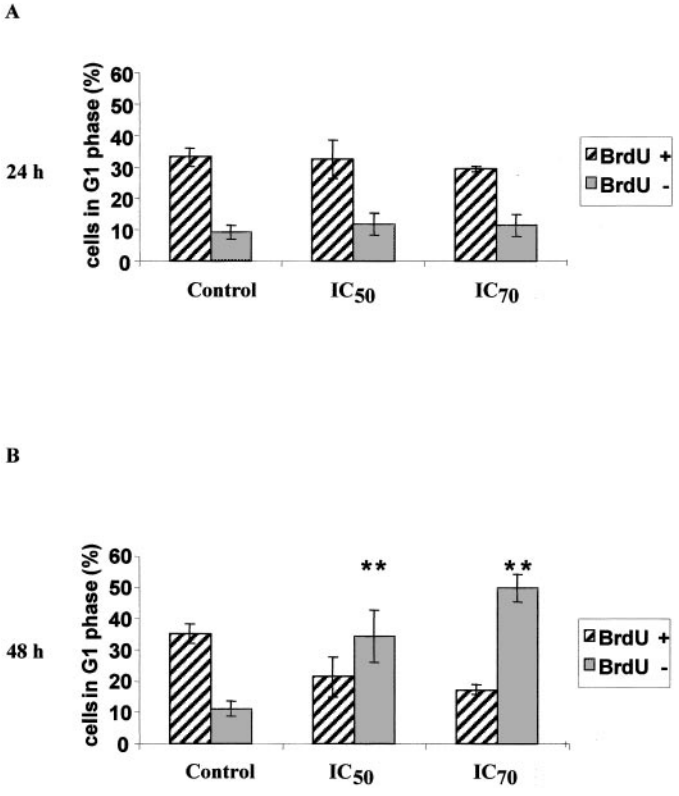

Fig. 4. Low concentrations of vinflunine induce a postmitotic G_1 arrest. Percentage of BrdU-labeled (BrdU+) or nonlabeled (BrdU−) cells in G_1 phase. Cells were treated with IC_{50} and IC_{70} of vinflunine for 24 h (A) or 48 h (B), and stained with BrdU and PI as described under *Materials and Methods*. BrdU+ cells result from their progression throughout the S phase, whereas BrdU− cells are blocked before the replication of DNA. Data are expressed as means ± S.D. from at three independent experiments.

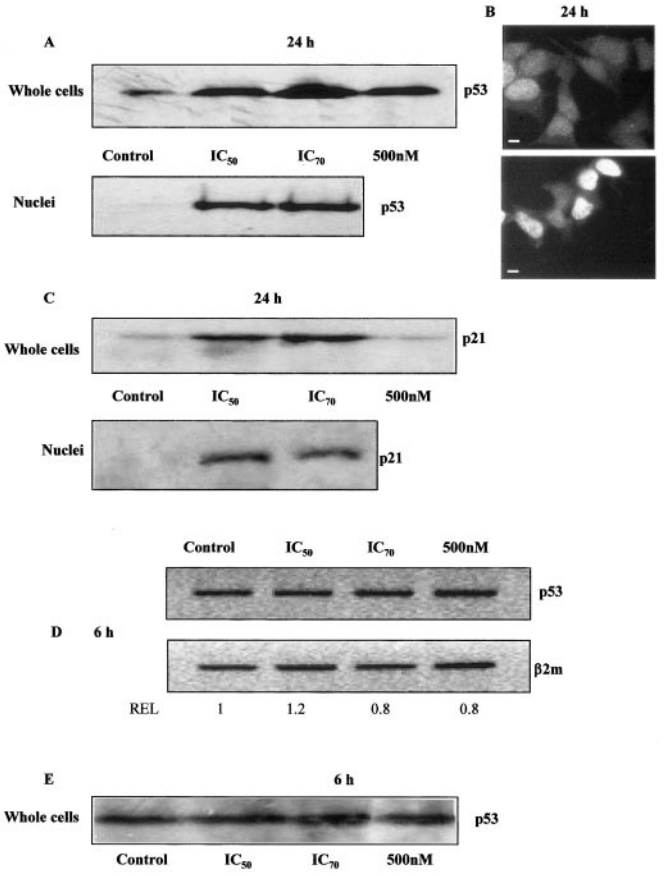

Fig. 5. The postmitotic G_1 arrest is associated with up-regulation of p53 and p21. A, immunoblots of whole cells and nuclear fractions analyzed with p53 antibody. The cells were incubated with IC_{50}, IC_{70}, or 500 nM vinflunine for 24 h. Cellular and nuclear lysates were obtained as described under *Materials and Methods*. B, distribution of p53 in control cells (top) or treated with IC_{50} of vinflunine (bottom) for 24 h. The cells were stained with p53 antibody and visualized by fluorescent microscopy. Scale bar, 5 μm. C, immunoblots of whole cells and nuclear fractions analyzed with p21 antibody. Treatment of the cells and extraction of cellular fractions were performed as described for p53. D, RT PCR of p53 RNA. The cells were treated with IC_{50}, IC_{70}, or 500 nM vinflunine for 6 h. E, immunoblot of whole cells analyzed with p53 antibody. The cells were incubated with IC_{50}, IC_{70}, or 500 nM vinflunine for 6 h. All these results are representative of at least three experiments.

flunine at low concentrations, p53 expression was quantified by Western blotting after a 24-h treatment. The IC_{50} and IC_{70} concentrations of vinflunine induced an increase in p53 expression in whole cells (Fig. 5A). However, neuroblastoma cells are known for their ability to inactivate p53 by sequestration in the cytoplasm (Ostermeyer et al., 1996; Moll et al., 1996). Thus, to determine whether p53 could act on SK-N-SH cell cycle progression, we investigated its nuclear translocation and the induction of its target, p21. By Western blotting analysis and immunofluorescence microscopy, we showed that p53 was translocated to the nucleus at the IC_{50} and IC_{70} concentrations of vinflunine at 24 h (Fig. 5, A and B). Moreover, expression of p21 was increased in whole cells and the protein was also translocated to nuclei (Fig. 5C). For the highest concentration used (500 nM), p53 was less well induced than at the IC_{70}, and p21 was not detected (Fig. 5, A and C). Because cells were massively blocked in mitosis at the high vinflunine concentration, nuclei could not be extracted for Western blotting. By immunofluorescence microscopy, p53 was distributed in the whole cell volume (data not shown). In addition, we confirm that modulation of the p53 levels did not occur during the first G_1-phase of the cell cycle; an increase of neither the p53 RNA level (Fig. 5D) nor the p53 protein expression (Fig. 5E) was observed after a 6-h treatment with vinflunine. Thus, after mitotic exit, the IC_{50} and IC_{70} concentrations of vinflunine induced a postmitotic G_1 arrest through an apparent p53-dependent pathway.

Mitochondria Seem to Be a Point of Convergence for the Apoptotic Signals Induced by Vinflunine at Low and High Concentrations. Mitochondria play a key role in apoptotic pathways by releasing several pro-apoptotic proteins such as cytochrome *c*. To study the potential involvement of mitochondria in vinflunine-induced apoptosis in the SK-N-SH cells, we investigated the release of cytochrome *c* in treated cells at low and high vinflunine concentrations. Immunofluorescence staining (Fig. 6A) showed that cytochrome *c* was released from mitochondria into the cytosol at all the vinflunine concentrations examined. In Fig. 6B, Western blotting of the cytosol extracted from cells treated with the IC_{50} and IC_{70} concentrations of vinflunine confirmed the cytochrome *c* release from mitochondria. Thus, mitochondria are involved in the apoptotic process induced by vinflunine, regardless of the cell cycle disturbance induced by the different concentrations of vinflunine.

It is known that mitochondrial permeabilization is modulated by Bcl-2 family members. The Bax/Bcl-2 ratio has been identified as having a critical role in apoptotic pathways induced by the Vinca alkaloids (Kawakami et al., 1999; Wall et al., 1999). Bax exhibits its proapoptotic effect after its translocation to mitochondrial membranes. The antiapoptotic protein Bcl-2 is constitutively present on mitochondria, and its inactivation by phosphorylation leads to a proapoptotic signal. Thus, we studied Bax and Bcl-2 expression and distribution by Western blotting. At low concentrations of vinflunine, Bax was up-regulated (data not shown) and translocated to mitochondria (Fig. 7A), whereas Bcl-2 expression remained constant (Fig. 7B). Thus, low concentrations of vinflunine, which induced a postmitotic G_1 arrest, displace the balance of mitochondrial Bcl-2-family members in favor of apoptosis. For the high vinflunine concentration, which induced mitotic block, Bax was not translocated to the mitochondria (Fig. 7A), and Bcl-2 was expressed at the same level as in control cells (Fig. 7B). In this case, the Bax/Bcl-2 ratio was not increased but Bcl-2 was phosphorylated (Fig. 7B), leading to a proapoptotic signal. Thus, whatever the studied concentration of vinflunine, Bcl-2-family proteins lead to a proapoptotic signal.

p53 has been described to play a nontranscriptional proapoptotic role. In fact, p53 can translocate to mitochondria, leading to the release of intermembrane space proapoptotic factors (Marchenko et al., 2000; Mihara et al., 2003). To investigate the potential role of p53 in SK-N-SH cells treated

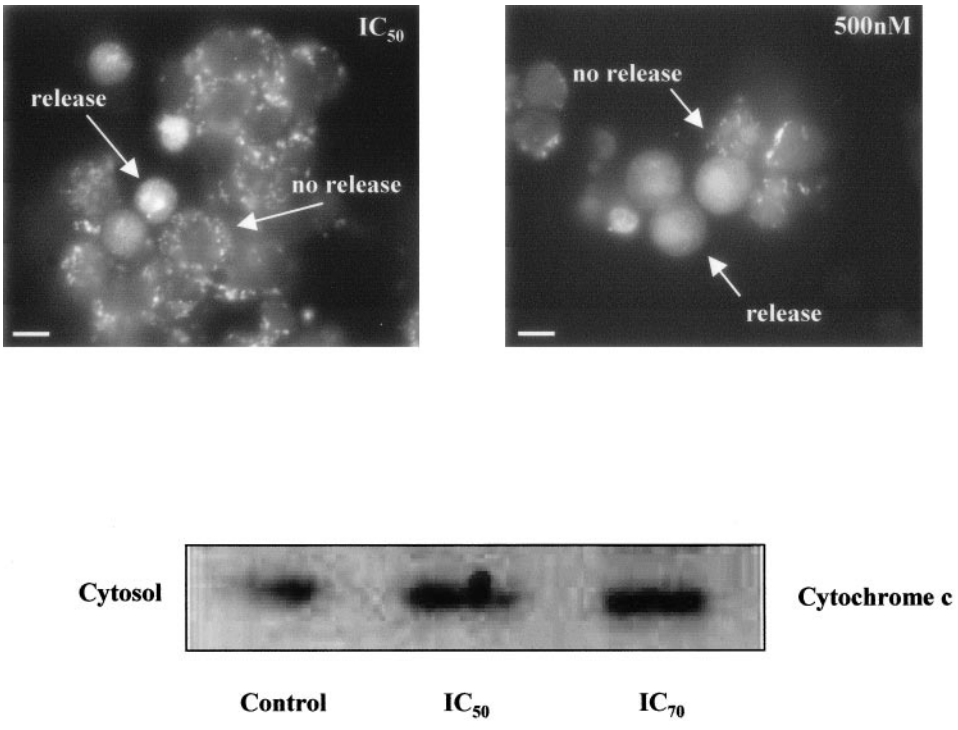

Fig. 6. Mitochondria are involved in apoptosis induced by vinflunine. Top, cytochrome *c* distribution visualization by fluorescent microscopy. The cells were treated with IC_{50} and 500 nM of vinflunine and stained with cytochrome *c* antibody. Cells with a released cytochrome *c* are different from those with nonreleased cytochrome *c* as shown in the pictures (as described previously in Andre et al., 2002). Results are representative of three independent experiments. Scale bar, 5 μm. Bottom, immunoblot of cytosols analyzed with cytochome *c* antibody. The cytosols were extracted as described under *Materials and Methods* from cells treated by IC_{50} and IC_{70} of vinflunine for 36 h.

with vinflunine, we looked for its presence on mitochondria. As shown in Fig. 7C, p53 translocated to mitochondria at all studied concentrations, with a slighter level for the high concentration of vinflunine.

Thus, mitochondria constitute the crossroads for apoptotic signals induced by both the low and high concentrations of vinflunine. The release of mitochondrial proapoptotic factors is regulated by modulation of the balance of the Bcl-2 family pro- and antiapoptotic members and probably by translocation of p53.

Vinflunine Behaves Similarly to Other Vinca Alkaloids on SK-N-SH Cells. To investigate whether the mechanism of apoptosis induction described with vinflunine may be extended to other Vinca alkaloids, we tested other drugs of this family on SK-N-SH cells, including vinblastine, the well known Vinca alkaloid (Fig. 8). The IC_{50} and IC_{70} concentrations of vinblastine and vinorelbine (2 and 3.7 nM and 13.5 and 30 nM, respectively) induced apoptosis (Fig. 8A) but induced neither a microtubule network depolymerization (Fig. 8B) nor a block in G_2/M (Fig. 8C). As described for vinflunine, the IC_{50} and IC_{70} concentrations of vinblastine induced a postmitotic G_1 arrest (increase in the percentage of BrdU unlabeled cells from 11.7 to 41.9% for control and IC_{70} concentration of vinblastine, respectively) (Fig. 8D). This arrest is associated with p53 up-regulation and nuclear translocation, and p21 up-regulation (Fig. 8E). The low concentrations of vinblastine also induced cytochrome *c* release from mitochondria (Fig. 8F), along with Bax up-regulation. High concentration of vinblastine (500 nM) induced a microtubule depolymerization, a G_2/M block (Fig. 8, B and C) and a Bcl-2 phosphorylation (Fig. 8G). Thus, the other Vinca alkaloids act on SK-N-SH cells similarly to vinflunine. Hence, our findings can be extended to the Vinca alkaloid family.

Discussion

The current study demonstrates a new mechanism of action of Vinca alkaloids at low concentrations on neuroblastoma cells. Low concentrations of vinflunine suppress microtubule dynamics and slow down mitotic progression but fail to block cells in G_2/M. Exiting from mitosis, cells undergo a p53-dependent postmitotic G_1 arrest, and the balance of mitochondrial Bcl-2 members is turned in favor of apoptosis. In contrast, high concentrations of vinflunine characteristically induce a G_2/M block and Bcl-2 phosphorylation. According to drug concentration, vinflunine induces apoptosis in human neuroblastoma cells by two different pathways that both converge to mitochondria (Fig. 9).

Vinflunine Suppresses Microtubule Dynamics in Living Neuronal Cells. Like other Vinca alkaloids, vinflunine suppresses microtubule dynamic instability in vitro but in a manner different than that of vinblastine (Ngan et al., 2001). Among Vinca alkaloids, only vinblastine has been studied for its effect on microtubule dynamics in living African green monkey kidney cells (BS-C-1; for review, see Jordan, 2002). In living SK-N-SH cells, vinflunine at its IC_{50} for cell growth at 72 h suppresses microtubule dynamic instability, mainly by affecting the rate and extent of both growing and shortening events. Such effect is similar to that observed for vinblastine in living BS-C-1 cells. However, at this low concentration, vinflunine failed to alter the time based catastrophe frequency (Jordan, 2002). Our results demonstrated, for the first time, that the newest Vinca alkaloid, vinflunine, suppresses microtubule dynamics in human neuronal cell type.

Vinca Alkaloids Can Act without G_2/M Block. It is largely accepted that Vinca alkaloids block cell cycle in G_2/M phase by depolymerizing microtubules and/or inhibiting their dynamics (Jordan, 2002). It is noteworthy that this mechanism depends on the drug, on its concentration, and on the cell type. For example, Blajeski et al. (2002) showed that, in some breast cancer cell lines, mitotic block was induced by low concentrations of vincristine and nocodazole, whereas a G_1 arrest appeared for high concentrations (Blajeski et al., 2002). Moreover, different types of G_1 block have been described with MDAs, mainly a pseudo G_1 arrest. In this case, cells exit from mitosis without undergoing cytokinesis and then block in an abnormal tetraploid G_1-like phase (Jordan et al., 1991, 1996). In addition, a premitotic diploid G_1 arrest has been described for low concentrations of paclitaxel (Taxol) (Giannakakou et al., 2001) or high concentration of vincristine and nocodazole (Blajeski et al., 2002). Finally, a postmitotic diploid G_1 arrest of cells treated with paclitaxel has been reported (Wahl et al., 1996).

It is known that p53 plays a key role in both G_1 and G_2/M arrest induced by MDAs. The p53 protein, and its target p21, are involved in the pseudo-G_1 arrest that occurs after a mitotic block, inhibiting the rereplication of DNA and the subsequent formation of 8N multinucleated cells (Notterman et al., 1998). Moreover, premitotic G_1 arrest observed with paclitaxel is also linked to p53 overexpression (Giannakakou et al., 2001).

In our study, cells treated by IC_{50} or IC_{70} concentrations of vinflunine do not block in G_2/M phase. They exit from mitosis

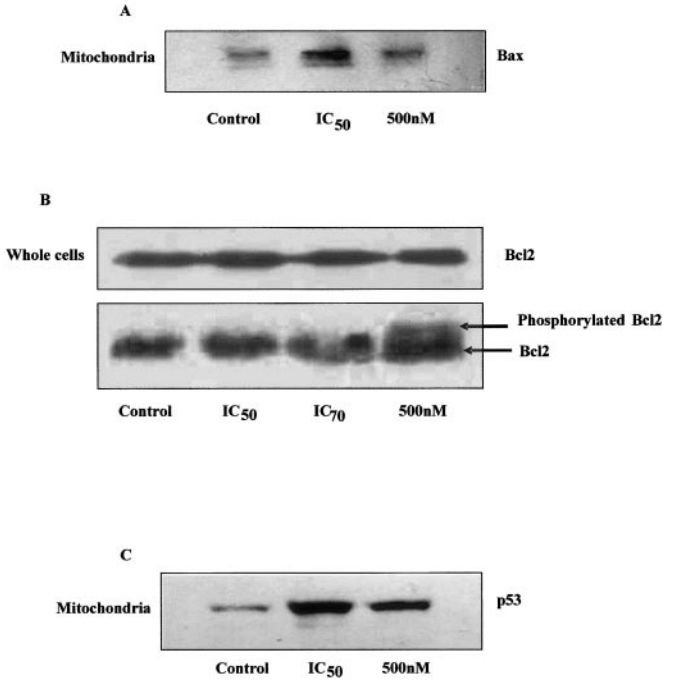

Fig. 7. Mitochondria constitute the point of convergence for apoptotic signals induced by vinflunine. Immunoblots of whole cells and mitochondrial fractions analyzed with Bax (A), total Bcl-2 and phosphorylated Bcl-2 (B), and p53 antibodies (C). The cells were incubated with IC_{50}, IC_{70}, or 500 nM vinflunine for 24 h before extraction of mitochondria as described under *Materials and Methods*. The immunoblots are representative of three independent experiments.

and undergo a postmitotic diploid G_1 arrest, with p53 and p21 involvement. In our knowledge, it is the first time that Vinca alkaloids are described to induce a postmitotic G_1 arrest.

How Does Suppression of Microtubule Dynamics Induced by Low Concentrations of Vinflunine Lead to Apoptosis in Neuroblastoma Cells? Even if the number of cells in mitosis was not significantly increased, the slowing down of the mitotic transition could trigger the subsequent G_1 arrest. Because we did not detect aneuploid cells, p53 activation and G_1 arrest cannot be explained by the abnormal segregation of chromosomes during an aberrant mitosis. This observation is in agreement with Chen and Horwitz (2002), who have shown that aneuploid cells were induced by microtubule-stabilizing drugs but not by microtubule-destabilizing agents. Thus, we can rather consider that the postmitotic G_1 arrest is caused by the activation of the spindle assembly checkpoint by low concentrations of vinflunine. These data strongly suggest that the slowing down of the metaphase-to-anaphase transition may result from the disruption of microtubule spindle functions through the suppression of their dynamics. This transient dysfunction of cells through mitosis may activate cell cycle regulators such as p53. Furthermore, the disturbance in mitosis progression could lead to minor DNA damages and thus to p53 activation, as suggested for paclitaxel by Wahl et al. (1996). In fact, these DNA injuries could be the consequence of a prolonged exposition of DNA to cellular damaging factors as reactive oxygen species, produced under Vinca alkaloid treatment (Groninger et al., 2002). Once induced, p53 is known to translocate to the nucleus to transactivate its target genes, resulting in G_1 arrest. However, SK-N-SH neuroblastoma cells are known to sequestrate p53 in cytosol, even after exposure to such DNA-damaging agents as doxorubicin (Moll et al., 1996). Giannakakou et al. (2002) showed that suppression of microtubule dynamics by paclitaxel enhanced p53 nuclear accumulation and activation of the p53 downstream target genes. Thus, in our model, suppression of microtubule dynamics by low concentrations of vinflunine is likely to lead to p53 nuclear translocation after exit of cells from mitosis.

Altogether, our results suggest that vinflunine, by acting on microtubule dynamics, disturbs mitosis progression, leading to induction of p53 expression. After the mitotic exit, suppression of microtubule dynamics also prevents p53 cyto-

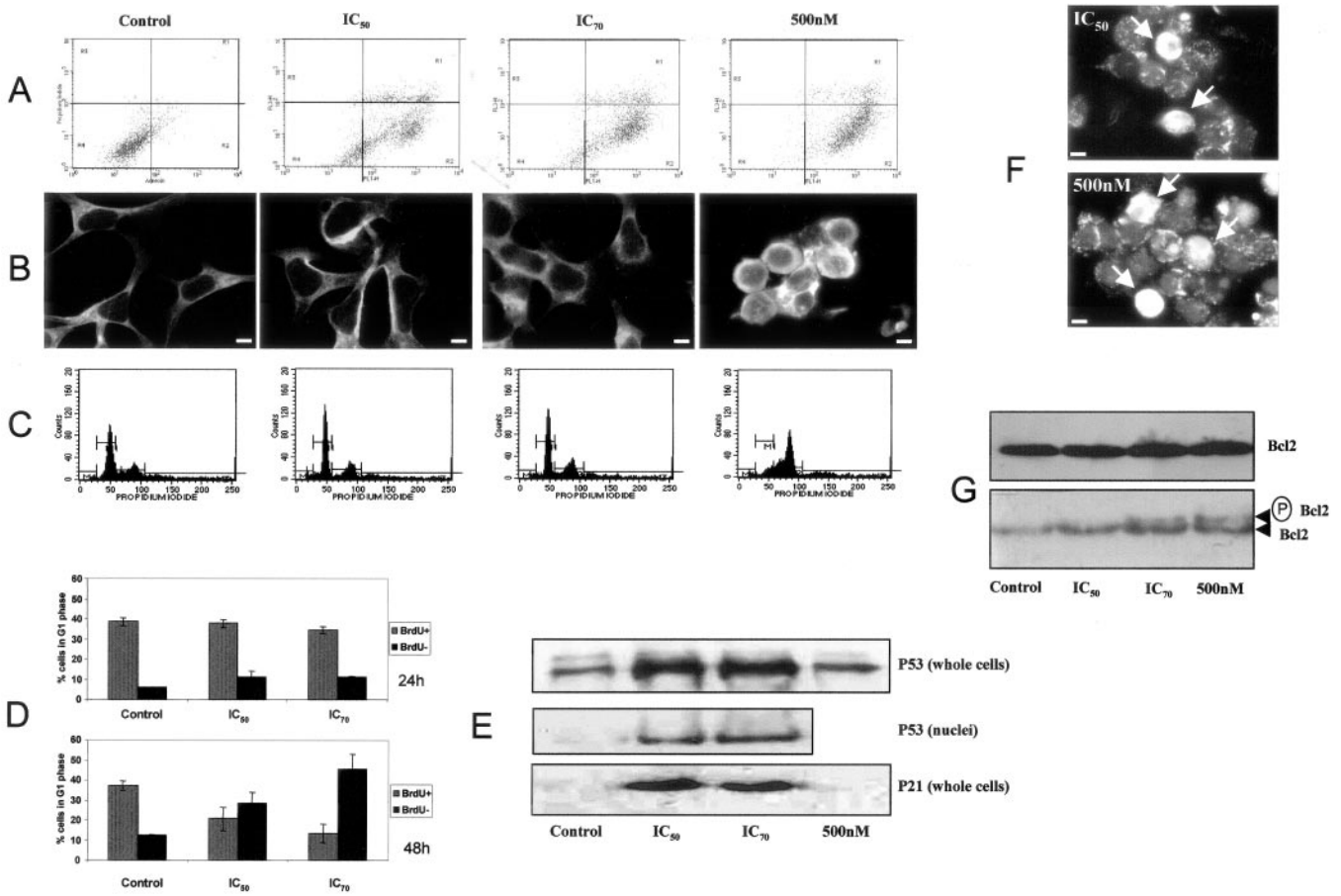

Fig. 8. Vinflunine acts as do other Vinca alkaloids on SK-N-SH cells. A, cytograms of cells treated by vinblastine for 72 h and stained with Annexin V-FITC and propidium iodide dual labeling. Apoptotic and late apoptotic cells are located in gates R1 and R2. B, microtubule network visualization by fluorescent microscopy. The cells were treated with IC_{50}, IC_{70}, or 500 nM vinblastine for 24 h and stained with α-tubulin antibody. Scale bar, 5 μm C, DNA distribution in cells treated with IC_{50}, IC_{70}, or 500 nM vinblastine for 24 h. Histograms and pictures are representative of three independent experiments. D, percentage of BrdU-labeled (BrdU+) or nonlabeled (BrdU−) cells in G_1 phase. Cells were treated with IC_{50} and IC_{70} of vinblastine for 24 h (top) or 48 h (bottom). E, immunoblots of whole cells and nuclear fractions analyzed with p53 and p21 antibody. The cells were incubated with IC_{50}, IC_{70}, or 500 nM vinblastine for 24 h. F, cytochrome *c* distribution visualization by fluorescent microscopy. The cells were treated with IC_{50} and 500 nM of vinblastine and stained with cytochrome *c* antibody. Cells with a released cytochrome *c* are indicated by an arrowhead. Scale bar, 5 μm. G, immunoblots of whole cells analyzed with Bcl-2 antibody. The cells were incubated with IC_{50}, IC_{70}, or 500 nM vinblastine.

plasmic sequestration and promotes p53 nuclear translocation, leading to p21 induction and to the postmitotic G_1 arrest.

Moreover, the p53-dependent G_1 arrest described above may be considered as a specific response of neuroblastoma model to Vinca alkaloid treatment. In fact, low concentrations of Vinca alkaloids induce a massive G_2/M block in non-neural cells, whatever their p53 status. Mammary HBL-100 cells, with a nonfunctional p53, and Lovo cells, with a wild p53, block both in G_2/M. In contrast, low concentrations of vinflunine fail to block in G_2/M the neuroblastoma cells SHEP, SH-SY5Y, and IMR32. This phenomenon may be linked to specific neuroblastoma oncogenes or to the ability of neuroblastoma cells to overexpress and/or sequestrate p53. Moreover, this sequestration is involved in neuroblastoma resistance to DNA-damaging agents, such as doxorubicin, and the combination of vinflunine with these drugs could be interesting for the clinical management of neuroblastomas that sequestrate p53.

Mitochondria Play a Key Role in Vinca Alkaloid-Induced Apoptosis Regardless of the Upstream Signal Pathway. We have demonstrated that apoptosis occurs by initiation of two distinct signal pathways by vinflunine, one induced by the low concentrations, after the p53-dependent postmitotic G_1 arrest, and the other induced by the high concentration after the canonical G_2/M arrest. Moreover, these two signal pathways converge to mitochondria to trigger the release of cytochrome *c* into cytosol.

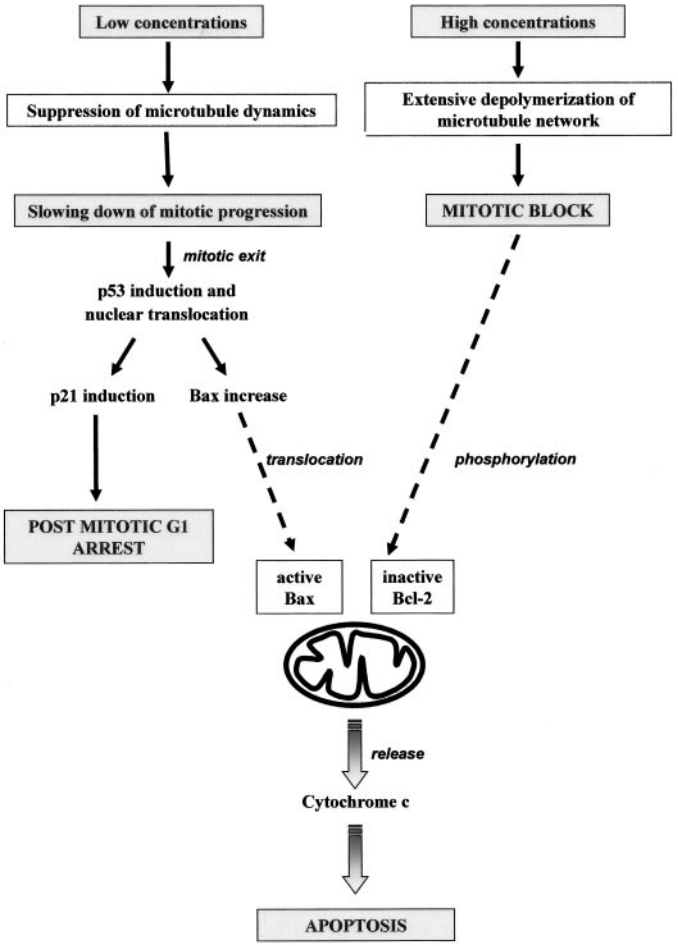

Fig. 9. Apoptotic pathways induced by Vinca alkaloids in neuroblastoma cells. Low concentrations of vinflunine suppress microtubule dynamics and slow mitotic progression but fail to block cells in G_2/M. Exiting from mitosis, cells undergo a p53-dependent postmitotic G_1 arrest, and the balance of mitochondrial Bcl-2 members is turned in favor of apoptosis. In contrast, high concentrations of vinflunine characteristically induce a G_2/M block and Bcl-2 phosphorylation. Regardless of the cell cycle effect, apoptotic pathways converge to mitochondria to induce cytochrome *c* release and then apoptosis.

The apoptogenic role of mitochondria was modulated by several elements in our model. First, we demonstrated that the Bcl-2-family proteins were differently involved according to disturbances of microtubule network organization and cell cycle progression. For the high concentrations of vinflunine that promote extensive microtubule depolymerization, the proapoptotic Bax protein was not increased on mitochondria. This absence might be explained by a microtubule-dependent trafficking of Bax. In addition, the antiapoptotic protein Bcl-2 was phosphorylated and thus it lost its antiapoptotic effect. This phosphorylation is likely to be linked to the mitotic block (Haldar et al., 1997). For the low concentrations of vinflunine, Bax increased on mitochondria whereas Bcl-2 remained constant. It is interesting that the Bax gene can be transactivated by p53 (Miyashita and Reed, 1995). Because we have shown that p53 was induced and translocated to the nucleus, a p53 transactivation of Bax gene might explain the proapoptotic mitochondrial signal induced by low concentrations of vinflunine. Finally, regardless of the concentration, the ratio of active Bax/active Bcl-2 increased, displacing the mitochondrial balance in favor of apoptosis.

A p53 nontranscriptional effect could also be involved in mitochondria permeabilization. In fact, death signals induce p53 protein localization to mitochondrial membranes, where it could have a direct proapoptotic role (Marchenko et al., 2000; Mihara et al., 2003). p53 can directly induce mitochondrial permeabilization and cytochrome *c* release by forming complexes with the antiapoptotic Bcl-2 family member Bcl-X_L. In SK-N-SH cells, we have shown that p53 translocated to mitochondria, and thus it may directly affect mitochondria to participate to the cytochrome *c* release process.

Finally, as demonstrated previously for paclitaxel and vinorelbine (Andre et al., 2000), a direct effect of vinflunine on mitochondria, probably via the mitochondrial tubulin (Carre et al., 2002) may occur because vinflunine induces the release of cytochrome *c* from mitochondria isolated from SK-N-SH cells (personal data).

In conclusion, our results highlight the key role of mitochondria in apoptosis induced by Vinca alkaloids. In addition, they show a new mechanism of apoptosis induction by Vinca alkaloids at low concentrations through suppression of microtubule dynamics and a p53-dependent postmitotic G_1 arrest, in neuroblastoma cells. Because those cells sequestrate p53 in a functional form in the cytoplasm, induction of its translocation to the nucleus by Vinca alkaloids could be an opportunity for the clinical management of this malignancy.

Acknowledgments

We thank Drs. Mary Ann Jordan and Leslie Wilson for invaluable help in learning the techniques of measuring microtubules dynamics, Eddy Pasquier, Nicolas André, and Daniel Lafitte for helpful discussion as well as Gérard Carles and Charles Prevôt for technical support. We also thank Drs. Vincent Peyrot and Pascale Barbier for tubulin purification and for help during tubulin labeling experi-

ments and Dr. Valérie Combaret for providing SHEP, SH-SY5Y, and IMR32 cell lines.

References

Andre N, Braguer D, Brasseur G, Goncalves A, Lemesle-Meunier D, Guise S, Jordan MA, and Briand C (2000) Paclitaxel induces release of cytochrome *c* from mitochondria isolated from human neuroblastoma cells. *Cancer Res* **60:**5349–5353.

Andre N, Carre M, Brasseur G, Pourroy B, Kovacic H, Briand C, and Braguer D (2002) Paclitaxel targets mitochondria upstream of caspase activation in intact human neuroblastoma cells. *FEBS Lett* **532:**256–260.

Barbier P, Gregoire C, Devred F, Sarrazin M, and Peyrot V (2001) In vitro effect of cryptophycin 52 on microtubule assembly and tubulin: molecular modeling of the mechanism of action of a new antimitotic drug. *Biochemistry* **40:**13510–13519.

Bennouna J, Fumoleau P, Armand JP, Raymond E, Campone M, Delgado FM, Puozzo C, and Marty M (2003) Phase I and pharmacokinetic study of the new vinca alkaloid vinflunine administered as a 10-min infusion every 3 weeks in patients with advanced solid tumours. *Ann Oncol* **14:**630–637.

Blajeski AL, Phan VA, Kottke TJ, and Kaufmann SH (2002) G_1 and G_2 cell-cycle arrest following microtubule depolymerization in human breast cancer cells. *J Clin Investig* **110:**91–99.

Carles G, Braguer D, Sabeur G, and Briand C (1998) The effect of combining antitubulin agents on differentiated and undifferentiated human colon cancer cells. *Anticancer Drugs* **9:**209–221.

Carre M, Andre N, Carles G, Borghi H, Brichese L, Briand C, and Braguer D (2002) Tubulin is an inherent component of mitochondrial membranes that interacts with the voltage-dependent anion channel. *J Biol Chem* **277:**33664–33669.

Chen JG and Horwitz SB (2002) Differential mitotic responses to microtubule-stabilizing and -destabilizing drugs. *Cancer Res* **62:**1935–1938.

Fan M, Goodwin M, Vu T, Brantley-Finley C, Gaarde WA and Chambers TC (2000) Vinblastine-induced phosphorylation of Bcl-2 and Bcl-XL is mediated by JNK and occurs in parallel with inactivation of the Raf-1/MEK/ERK cascade. *J Biol Chem* **275:**29980–29985.

Giannakakou P, Robey R, Fojo T, and Blagosklonny MV (2001) Low concentrations of paclitaxel induce cell type-dependent p53, p21 and G_1/G2 arrest instead of mitotic arrest: molecular determinants of paclitaxel-induced cytotoxicity. *Oncogene* **20:**3806–3813.

Giannakakou P, Nakano M, Nicolaou KC, O'Brate A, Yu J, Blagosklonny MV, Greber UF, and Fojo T (2002) Enhanced microtubule-dependent trafficking and p53 nuclear accumulation by suppression of microtubule dynamics. *Proc Natl Acad Sci USA* **99:**10855–10860.

Glaser T and Weller M (2001) Caspase-dependent chemotherapy-induced death of glioma cells requires mitochondrial cytochrome *c* release. *Biochem Biophys Res Commun* **281:**322–327.

Gonçalves A, Braguer D, Carles G, Andre N, Prevot C, and Briand C (2000) Caspase-8 activation independent of CD95/CD95-L interaction during paclitaxel-induced apoptosis in human colon cancer cells (HT29–D4). *Biochem Pharmacol* **60:**1579–1584.

Gonçalves A, Braguer D, Kamath K, Martello L, Briand C, Horwitz S, Wilson L, and Jordan MA (2001) Resistance to Taxol in lung cancer cells associated with increased microtubule dynamics. *Proc Natl Acad Sci USA* **98:**11737–11742.

Groninger E, Meeuwsen-De Boer GJ, De Graaf SS, Kamps WA, and De Bont ES (2002) Vincristine induced apoptosis in acute lymphoblastic leukaemia cells: a mitochondrial controlled pathway regulated by reactive oxygen species? *Int J Oncol* **21:**1339–1345.

Haldar S, Basu A, and Croce CM (1997) Bcl-2 is the guardian of microtubule integrity *Cancer Res* **57:**229–233.

Honoré S, Kamath K, Braguer D, Wilson L, Briand C, and Jordan MA (2003) Suppression of microtubule dynamics by discodermolide by a novel mechanism is associated with mitotic arrest and inhibition of tumor cell proliferation. *Mol Cancer Ther* **12:**1303–1311.

Hyman A, Drechsel D, Kellogg D, Salser S, Sawin K, Steffen P, Wordeman L, and Mitchison T (1991) Preparation of modified tubulins. *Methods Enzymol* **196:**478–485.

Jean-Decoster C, Brichese L, Barret JM, Tollon Y, Kruczynski A, Hill BT, and Wright M (1999) Vinflunine, a new vinca alkaloid: cytotoxicity, cellular accumulation and action on the interphasic and mitotic microtubule cytoskeleton of PtK2 cells. *Anticancer Drugs* **10:**537–543.

Jordan MA, Thrower D, and Wilson L (1991) Mechanism of inhibition of cell proliferation by Vinca alkaloids. *Cancer Res* **51:**2212–2222.

Jordan MA, Wendell K, Gardiner S, Derry WB, Copp H, and Wilson L (1996) Mitotic block induced in HeLa cells by low concentrations of paclitaxel (Taxol) results in abnormal mitotic exit and apoptotic cell death. *Cancer Res* **56:**816–825.

Jordan MA (2002) Mechanism of action of antitumor drugs that interact with microtubules and tubulin. *Curr Med Chem Anti-Cancer Agents* **2:**1–17.

Kawakami K, Tsukuda M, Mizuno H, Nishimura G, Ishii A, and Hamajima K (1999) Alteration of the Bcl-2/Bax status of head and neck cancer cell lines by chemotherapeutic agents. *Anticancer Res* **19:**3927–3932.

Kruczynski A, Barret JM, Etievant C, Colpaert F, Fahy J, and Hill BT (1998) Antimitotic and tubulin-interacting properties of vinflunine, a novel fluorinated Vinca alkaloid. *Biochem Pharmacol* **55:**635–648.

Kruczynski A and Hill BT (2001) Vinflunine, the latest Vinca alkaloid in clinical development. A review of its preclinical anticancer properties. *Crit Rev Oncol Hematol* **40:**159–173.

Kruczynski A, Etievant C, Perrin D, Chansard N, Duflos A, and Hill BT (2002) Characterization of cell death induced by vinflunine, the most recent Vinca alkaloid in clinical development. *Br J Cancer* **86:**143–150.

Liu XM, Wang LG, Kreis W, Budman DR, and Adams LM (2001) Differential effect of vinorelbine versus paclitaxel on ERK2 kinase activity during apoptosis in MCF-7 cells. *Br J Cancer* **85:**1403–1411.

Lobert S, Ingram JW, Hill BT, and Correia JJ (1998) A comparison of thermodynamic parameters for vinorelbine- and vinflunine-induced tubulin self-association by sedimentation velocity. *Mol Pharmacol* **53:**908–915.

Marchenko ND, Zaika A, and Moll UM (2000) Death signal-induced localization of p53 protein to mitochondria. A potential role in apoptotic signaling. *J Biol Chem* **275:**16202–16212.

Mejillano MR and Himes RH (1989) Tubulin dimer dissociation detected by fluorescence anisotropy. *Biochemistry* **28:**6518–6524.

Mihara M, Erster S, Zaika A, Petrenko O, Chittenden T, Pancoska P, and Moll UM (2003) p53 has a direct apoptogenic role at the mitochondria. *Mol Cell* **11:**577–590.

Miyashita T and Reed JC (1995) Tumor suppressor p53 is a direct transcriptional activator of the human bax gene. *Cell* **80:**293–299.

Moll UM, Ostermeyer AG, Haladay R, Winkfield B, Frazier M, and Zambetti G (1996) Cytoplasmic sequestration of wild-type p53 protein impairs the G_1 checkpoint after DNA damage. *Mol Cell Biol* **16:**1126–1137.

Ngan VK, Bellman K, Panda D, Hill BT, Jordan MA, and Wilson L (2000) Novel actions of the antitumor drugs vinflunine and vinorelbine on microtubules. *Cancer Res* **60:**5045–5051.

Ngan VK, Bellman K, Hill BT, Wilson L, and Jordan MA (2001) Mechanism of mitotic block and inhibition of cell proliferation by the semisynthetic Vinca alkaloids vinorelbine and its newer derivative vinflunine. *Mol Pharmacol* **60:**225–232.

Notterman D, Young S, Wainger B, and Levine AJ (1998) Prevention of mammalian DNA reduplication, following the release from the mitotic spindle checkpoint, requires p53 protein, but not p53-mediated transcriptional activity. *Oncogene* **17:**2743–2751.

Ostermeyer AG, Runko E, Winkfield B, Ahn B, and Moll UM (1996) Cytoplasmically sequestered wild-type p53 protein in neuroblastoma is relocated to the nucleus by a C-terminal peptide. *Proc Natl Acad Sci USA* **93:**15190–15194.

Toso RJ, Jordan MA, Farrell KW, Matsumoto B, and Wilson L (1993) Kinetic stabilization of microtubule dynamic instability in vitro by vinblastine. *Biochemistry* **32:**1285–1293.

Wahl AF, Donaldson KL, Fairchild C, Lee FY, Foster SA, Demers GW, and Galloway DA (1996) Loss of normal p53 function confers sensitization to Taxol by increasing G_2/M arrest and apoptosis. *Nat Med* **2:**72–79.

Wall NR, Mohammad RM, and Al-Katib AM (1999) Bax:Bcl-2 ratio modulation by bryostatin 1 and novel antitubulin agents is important for susceptibility to drug induced apoptosis in the human early pre-B acute lymphoblastic leukemia cell line, Reh. *Leuk Res* **23:**881–888.

Address correspondence to: Dr. Diane Braguer, FRE-CNRS 2737, UFR Pharmacie, 27 boulevard Jean Moulin, 13385 Marseilles cedex 05, France. E-mail: diane.braguer@pharmacie.univ-mrs.fr